Leukemia (2014) **28**, 278–288

www.nature.com/leu

ORIGINAL ARTICLE

Therapeutic antibody targeting of Notch1 in T-acute lymphoblastic leukemia xenografts

V Agnusdei[1,6], S Minuzzo[2,6], C Frasson[3], A Grassi[1], F Axelrod[4], S Satyal[4], A Gurney[4], T Hoey[4], E Seganfreddo[3], G Basso[3], S Valtorta[5], RM Moresco[5], A Amadori[1,2] and S Indraccolo[1]

T-acute lymphoblastic leukemia (T-ALL) is characterized by several genetic alterations and poor prognosis in about 20–25% of patients. Notably, about 60% of T-ALL shows increased Notch1 activity, due to activating *NOTCH1* mutations or alterations in the *FBW7* gene, which confer to the cell a strong growth advantage. Therapeutic targeting of Notch signaling could be clinically relevant, especially for chemotherapy refractory patients. This study investigated the therapeutic efficacy of a novel anti-Notch1 monoclonal antibody by taking advantage of a collection of pediatric T-ALL engrafted systemically in NOD/SCID mice and genetically characterized with respect to *NOTCH1/FBW7* mutations. Anti-Notch1 treatment greatly delayed engraftment of T-ALL cells bearing Notch1 mutations, including samples derived from poor responders or relapsed patients. Notably, the therapeutic efficacy of anti-Notch1 therapy was significantly enhanced in combination with dexamethasone. Anti-Notch1 treatment increased T-ALL cell apoptosis, decreased proliferation and caused strong inhibitory effects on Notch-target genes expression along with complex modulations of gene expression profiles involving cell metabolism. Serial transplantation experiments suggested that anti-Notch1 therapy could compromise leukemia-initiating cell functions. These results show therapeutic efficacy of Notch1 blockade for T-ALL, highlight the potential of combination with dexamethasone and identify surrogate biomarkers of the therapeutic response.

Leukemia (2014) **28,** 278–288; doi:10.1038/leu.2013.183

Keywords: Notch1; T-ALL; apoptosis; targeted therapy; predictive biomarkers

INTRODUCTION

T-acute lymphoblastic leukemia (T-ALL) shows increased Notch1 activity in about 60% of cases.[1,2] Constitutive activation of this signaling pathway confers to the cell a strong growth advantage, due to the fact that Notch1 directly controls key regulators of cell proliferation and metabolism.[3–6] Previous attempts to target Notch signaling in T-ALL were largely based on administration of gamma-secretase inhibitors (GSI), which block cleavage of Notch receptors. However, GSI exhibit significant toxicity due to the development of severe secretory diarrhea[7] as a consequence of simultaneous inhibition of Notch1 and Notch2 signaling in gut epithelial stem cells.[8,9] Recently, antibodies that inhibit signaling of both normal and mutated Notch1 receptors have been characterized.[10,11] These studies found that anti-Notch1 antibodies effectively block Notch signaling *in vitro* and subcutaneous growth of tumor xenografts bearing Notch1 mutations,[11] but their potential therapeutic activity was not evaluated in patient-derived, pre-clinical models of Notch-dependent hematological malignancies. Here we investigated the therapeutic effects of a novel human Notch1-specific monoclonal antibody (mAb) in various T-ALL xenografts obtained from patients resistant to conventional treatment, analyzed the mechanisms involved and identified predictive biomarkers of response.

MATERIALS AND METHODS

T-ALL xenografts establishment and tumorigenicity assay

Primary T-ALL cells (PDTALL) were obtained from the bone marrow (BM) of newly diagnosed ALL pediatric patients, according to the guidelines of the local ethics committee. For initial xenografts establishment, 6- to 9-weeks-old mice were injected intravenously (i.v.) with 1×10^7 T-ALL cells in 300 μl of Dulbecco's phosphate buffered saline. Secondary transplants were obtained by injecting 5×10^6 T-ALL cells per mouse. NOD/SCID mice were purchased from Charles River (Wilmington, MA, USA). Procedures involving animals and their care conformed with institutional guidelines that comply with national and international laws and policies (EEC Council Directive 86/609, OJ L 358, 12 December, 1987) and were authorized by the local ethical committee. T-ALL cell engraftment was monitored by periodic blood drawings and flow cytometric analysis of CD5 and CD7 markers over a 5-month period. Details of *NOTCH1* and *FBW7* mutational analysis can be found in Supplementary Data. To test the effect of Notch1 blockade on leukemia engraftment, NOD/SCID mice were intraperitoneally (i.p.) injected with the humanized anti-human Notch1 mAb OMP-52M51 (Oncomed Pharmaceuticals Inc., Redwood, CA, USA) or control humanized antibody (Rituximab, Roche, Basel, Switzerland), both used at 20 mg/Kg, 2 days after i.v. injection of T-ALL cells. Anti-Notch1 or control antibody was subsequently administered weekly for an average of three doses (6 mice/group). In the late intervention trial, administration of OMP-52M51 started 11 days after leukemia cell injection, followed by a second dose 1 week later. Dexamethasone was administered i.p. at 10 mg/Kg daily from day 11 to day 15 and from day 18 until day 20. In all the experiments, mice were inspected

[1]UOC Immunologia e Diagnostica Molecolare Oncologica, Istituto Oncologico Veneto—IRCCS, Padova, Italy; [2]Dipartimento Scienze Chirurgiche, Oncologiche e Gastroenterologiche -Sez. Oncologia e Immunologia, Università di Padova, Padova, Italy; [3]Oncohematology Laboratory, Department of Woman and Child Health, Università di Padova, Padova, Italy; [4]OncoMed Pharmaceuticals Inc., Redwood City, CA, USA and [5]Nuclear Medicine Department, San Raffaele Scientific Institute; Fondazione Tecnomed, University of Milan Bicocca; IBFM-CNR, Milan, Italy. Correspondence: Dr S Indraccolo, UOC Immunologia e Diagnostica Molecolare Oncologica, Istituto Oncologico Veneto—IRCCS, via Gattamelata, 64, Padua I-35128, Italy.
E-mail: stefano.indraccolo@unipd.it
[6]These authors contributed equally to this work.
Received 6 February 2013; revised 18 May 2013; accepted 12 June 2013; accepted article preview online 18 June 2013; advance online publication, 23 July 2013

Table 1. T-ALL patient and xenograft features

Sample ID	*Age*	*Phenotype*	*MRD risk*	*PGR/PPR*	*TCR rearrangements*			*NOTCH1 status*	*FBW7 status*
PDTALL6	13	T int	MR	PGR	Vg7Jg1.1	Vg1Jg1.3	Vd1Jd1	wt	wt
PDTALL9	9	Early T	HR	(deceased)	Vd1Jd1	TalDb1	Vg5Jg1.3	wt	wt
PDTALL13	5	T	HR	(deceased)	Vg2Jg2.3	Vb29Jb2.7		wt	wt
PDTALL14	8	Int/mat	MR	PPR	Vg4Jg2.3	Vg8Jg2.3	Vb10Jb2.1	wt	wt
PDTALL15	7	T	HR	PPR	Vb5.1Jb2.1	Vg9Jg2.3		wt	wt
PDTALL16	5	T mat	MR	PPR	Vg3Jg2.3	Vb21.3Jb2.1		wt	wt
PDTALL18	6	T int	MR	PPR	Vg4Jg2.3	Vg2Jg2.3	Vb6.1Jb2.7	wt	wt
PDTALL1	12	T int	SR	PGR	Vd1Jd1	Vb13.5Jb1.1	Vg10Jg2.3	HD mut. (T5039A (heterozygous) => L1678Q (heterozygous))	Exon9 C1542T R465C heterozygous
PDTALL4	NA	T	MR	PGR	Vg10Jg2.3	Vg2Jg1.3		HD mut. (T5027A (heterozygous) => V1677D (heterozygous))	Exon9 G1543A R465C heterozygous
PDTALL7	5	T int	MR	PGR	Vb8Jb1.6	Dd2Jb2.1		HD mut. (T5033C (heterozygous) => L1679P (heterozygous))	wt
PDTALL10	10	Early T	MR	PGR	Vg4Jg2.3	Db1Jb1.4		HD mut. (T4799C => L1601P; G4823A => R1609H)	Exon9 C1542T R465C heterozygous
PDTALL11	6	Thym	MR	PPR	Vb5 Jb2.1	Vb19Jb2.7		HD mut. (T5033A => L1679P)	wt
PDTALL20	11	T int	HR	PGR	Vg8Jg2.1	Db1Jb2.5	Vg8Jg2.3	HD mut. (L1677 => P)	wt
PDTALL21	9	T int	MR	PGR	NA	NA		HD mut. (in frame 4852 del <CCCTAC> ins <TTTCCGCGGATGGGC> => 1618 PY< FPRMG (heterozygous))	wt
PDTALL5	2	T int	MR	PGR	Vg2Jg2.1	Db2Jb2.2		PEST mut. (7538 ins <T> (heterozygous) => 2513 SPE > FP*STOP (heterozygous))	wt
PDTALL12	4	Early T	MR	PGR	Vd1Jd1	TalDb1		PEST mut.	wt
PDTALL22	16	Early T	MR	PGR	Vb11Jb2.5	Db1Jb1.2	Vg2Jg1.3	PEST mut. (in frame 7328 ins <GTTGATG> => V2443G*STOP (heterozygous))	wt
PDTALL8	3	T int	MR	PPR	Vd1Jd1	Db1Jb1.1		HD + PEST mut. (4742 del <C> ins <TGATGCC> => P1581*STOP (heterozygous); 7356 ins <TTAGTAGCC> => V2453*STOP)	wt
PDTALL19	16	Early T	MR	Relapse PPR	DH6JH4	Vg11Jg1.3		HD + TAD mut. (in frame 4818 ins <GGT> => 1606 P < LV (heterozygous); in frame 7262 ins < GGGGCCCG> => V2421GGP*STOP	Exon9 V444 => D

Abbreviations: HD, heterodimerization domain; HR, high risk; MR, medium risk; MRD, minimal residual disease risk; mut., mutated; NA, not available; PEST, proline-glutamic acid-serine-threonine-rich domain; PGR, prednisone good responder, PPR, prednisone poor responder; SR, standard risk; TAD, C-terminal transcription activation domain; TCR, T-cell receptor; wt, wild type. 19 pediatric T-ALL patients were classified for phenotype, risk (according to the minimal residual disease risk classification) and response to therapy. Patient age range was 2-16 years. Genomic DNA obtained from T-ALL xenografts was analyzed in order to compare TCR rearrangements in matched patients and to identify possible mutations in NOTCH1 or FBW7 genes.

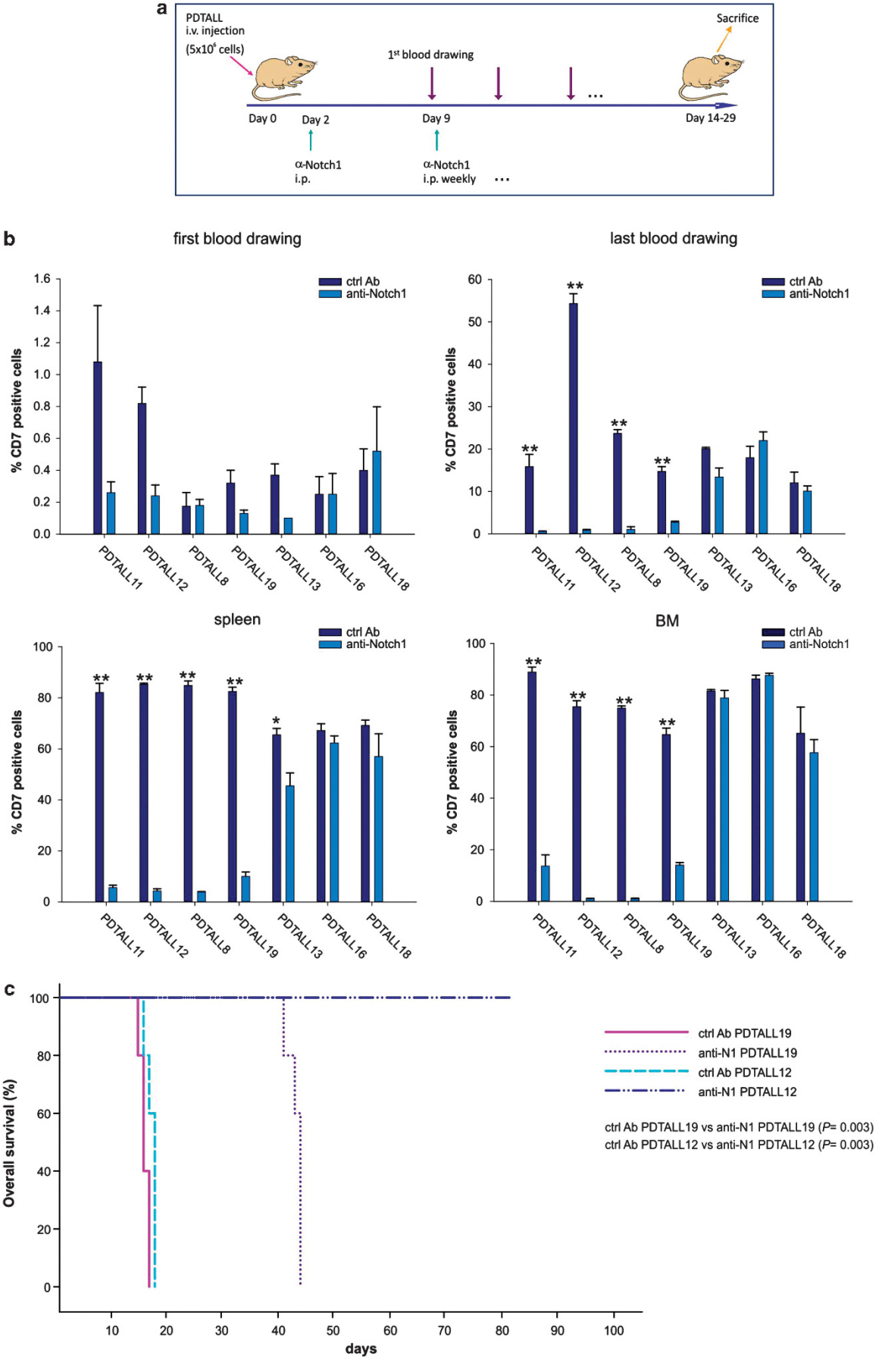

twice weekly to detect early signs and symptoms of leukemia, and blood was drawn to measure T-ALL cell engraftment.

Cytofluorimetric analysis and cell sorting

Fluorescein isothiocyanate-labeled mAb against CD5 and phycoerythrin-Cy5-labeled mAb against CD7 (Coulter, Fullerton, CA, USA) were used for the detection of T-ALL cells in mouse samples. Apoptosis evaluation was performed by the Annexin-V-FLUOS Staining Kit (Roche Diagnostics, Penzberg, Germany). Proliferation was evaluated by the AlexaFluor 488-labeled Ki67 staining kit (BD Biosciences, San Jose, CA, USA). Samples were analyzed on the Beckman Coulter EPICS-XL Flow Cytometer (Coulter) or BD LSRII Flow Cytometer (BD Biosciences). T-ALL cells from the BM and spleen were incubated with phycoerythrin-Cy5-conjugated antibody against human CD5 and sorted on a BD FACS Aria III cell sorter (BD Biosciences). Relative percentages of the $CD5^+$ subpopulation were calculated based on viable gated cells (as indicated by physical parameters, side scatter and forward scatter). After sorting, an aliquot of the sorted cells was used to check the purity of the population.

Reverse transcription-PCR and quantitative PCR (qPCR)

Total RNA was isolated using TRIzol Reagent (Life Technologies, Paisley, UK) according to the manufacturer's instructions. cDNA was synthesized from 1 to 1.5 μg of total RNA using the High Capacity RNA-to-cDNA kit (Life Technologies). For qPCR analysis, the SYBR Green dye and ABI Prism 7900 Sequence Detection System were used (both from Life Technologies). Relative quantification was done using the ΔΔCt method, normalizing to β2-microglobulin mRNA. Primers used for qPCR analysis are: CR2-for: 5′-CTGCGGTTCAGTGTCCACAT-3′; CR2-rev: 5′-GGTGAAGCCAAACATGCAAG C-3′; DTX-1-for: 5′-GTGGGCTGATGCCTGTGAAT-3′; DTX-1-rev: 5′-CGAGCGTC CTCCTTCAGCAC-3′; HES1-for: 5′-GGCGGCTAAGGTGTTTGGAG-3′; HES-1 rev: 5′-GGAAGGTGACACTGCGTTGG-3′; NOTCH3-for: 5′-CAAGGGTGAGAGCCTG ATGG-3′; NOTCH3-rev: 5′-GAGTCCACTGACGGCAATCC-3′; pTa-for: 5′-ATGG TGGTGGTCTGCCTGGT-3′; pTa-rev: 5′-AGTTGGTCCAGGTGCCATCC-3′; β2-microglobulin-for 5′-TGCTGTCTCCATGTTTGATGTATCT-3′; and β2-micro-globulin-rev: 5′-TCTCTGCTCCCCACCTCTAAGT-3′.

For analysis of the Notch pathway activation, 21 Notch-target genes were evaluated in duplicates by Custom TaqManArray Cards (Supplementary Table SI) using the TaqMan Universal PCR Master Mix (Life Technologies) and ABI Prism 7900 Sequence Detection System. Relative quantification was done using the ΔΔCt method, normalizing to β2-microglobulin mRNA.

Western blot analysis

Cell lysates were run on 4–12% polyacrylamide gels; separated proteins were then blotted for 2 h at 400 mA onto a nitrocellulose membrane. Immunoprobing was performed using rabbit mAb against PARP (poly ADP-ribose polymerase; Cell Signaling Technologies, Beverly, MA, USA), followed by hybridization with a horseradish peroxidase-conjugated anti-rabbit Ab (Amersham-Pharmacia, Little Chalfont, UK). Antigens were identified by luminescent visualization using the SuperSignal kit (Pierce, Rockford, IL, USA).

Preparation of cRNA, GeneChip microarray analysis and data normalization

Total RNA was isolated using TRIzol Reagent (Life Technologies) according to the manufacturer's instructions. Sense-strand cDNA from total RNA was prepared using the Ambion WT Expression Kit (Life Technologies). The cDNA was then fragmented and labeled using the Affymetrix GeneChip WT Terminal Labeling kit (Affymetrix, Santa Clara, CA, USA). Total RNA and cRNA quality was controlled by Agilent RNA 6000 Nano Kit and Agilent 2100 Bioanalyzer (Agilent Technologies, Santa Clara, CA, USA). cDNA was quantified by ND-1000 Spectrophotometer (NanoDrop Technologies, Wilmington, DE, USA). Labeled sense-strand cDNA was used for screening of GeneChip Human Exon 1.0 ST Array (Affymetrix). Three independent experiments were performed. Each biological replicate consisted of T-ALL cells from the BM of different mice that were pooled before sorting and RNA extraction ($n = 3$–6 samples per pool). Hybridization and scanning were conducted on the Affymetrix platform. Further experimental details can be found under Supplementary Data.

Optical imaging of tumors

To perform *in vivo* imaging, leukemia cells were transduced by a lentiviral vector encoding the *Luciferase* reporter gene, and bioluminescence images were acquired on IVIS Imaging System (Xenogen Corporation, Alameda, CA, USA) as described before.[12]

Statistical analysis

Results were expressed as mean value ± s.d. Statistical analysis of data was performed using the Student's *t*-test. Mouse survival was calculated using the Kaplan–Meier method, and survival curves were compared by a log-rank test. Differences were considered statistically significant when $P \leqslant 0.05$.

RESULTS

Development and characterization of a novel anti-human Notch1 Ab

In an effort to find an optimal Notch1 antagonist antibody, we generated large panels of monoclonal antibodies against various regions of the extracellular domain of human Notch1. These antibodies were tested for activity in ligand-dependent reporter gene assays and active antibodies were then tested *in vivo* in T-ALL xenograft models. From this effort, we identified OMP-52M51 as a potent Notch1 antagonist. OMP-52M51 was generated by immunizing mice with a fragment of human Notch1 protein consisting of the LNR (lin12-Notch repeats) plus HD (heterodimerization) domains of human Notch1.[13] We found that OMP-52M51 efficiently blocked Notch1 signaling driven in response to DLL4 (delta-like ligand 4), Jagged 1 or Jag2 (Supplementary Figure S1). We also found that OMP-52M51 could reduce the levels of Notch1 intracellular domain in the HPB-ALL cell line, which contains activating mutations in Notch1[2] (Supplementary Figure S2A) and significantly blocks HPB-ALL growth in an *in vivo* subcutaneous xenograft model (Supplementary Figure S2B).

Generation and characterization of T-ALL xenografts from leukemia patients

To further evaluate the therapeutic utility of OMP-52M51, we sought to assess its activity in a panel of patient-derived xenograft models established from clinical samples. With this concept in mind, we initially aimed to establish leukemia xenografts in NOD/SCID mice. Following i.v. injection of T-ALL cells (1×10^7 cells/mouse) freshly obtained from the clinic, engraftment rate was 52% after a 5-month observation period and we obtained a collection of $n = 19$ xenografts that could be passaged to serial mouse recipients. There was no difference in the phenotype and minimal residual disease (MRD) risk classifications between

Figure 1. Anti-Notch1 inhibits the growth of Notch1-driven T-ALL xenografts. (**a**) Outline of treatment with anti-Notch1 (OMP-52M51) or control antibody (ctrl Ab; Rituximab). NOD/SCID mice ($n = 6$ mice/group) were i.p. treated with anti-Notch1 or ctrl Ab 2 days after i.v. injection of T-ALL cells (5×10^6 cells/mouse). Antibodies were subsequently administered at weekly intervals at 20 mg/Kg. Leukemia engraftment was tracked by serial blood drawings and flow cytometric analysis. (**b**) Measurement of circulating blasts by flow cytometry after first blood drawing, 9–11 days from the beginning of the experiment (left panel, top). The last blood drawing was obtained at killing, when initial signs of illness appeared in control mice (right panel, top). Quantification of leukemia cells in the spleen (left panel, bottom) and the BM (right panel, bottom) was carried out at killing. Statistically significant differences are indicated (*$P < 0.05$; **$P < 0.001$). Genetic status of the T-ALL xenografts: PDTALL8, 11, 12 and 19 were NOTCH1-mutated samples, whereas PDTALL13, 16 and 18 xenografts had wild-type Notch1 receptors. (**c**) Kaplan–Meier survival curves of leukemic mice (PDTALL12 and PDTALL19 xenografts) after treatment with anti-Notch1 or ctrl Ab.

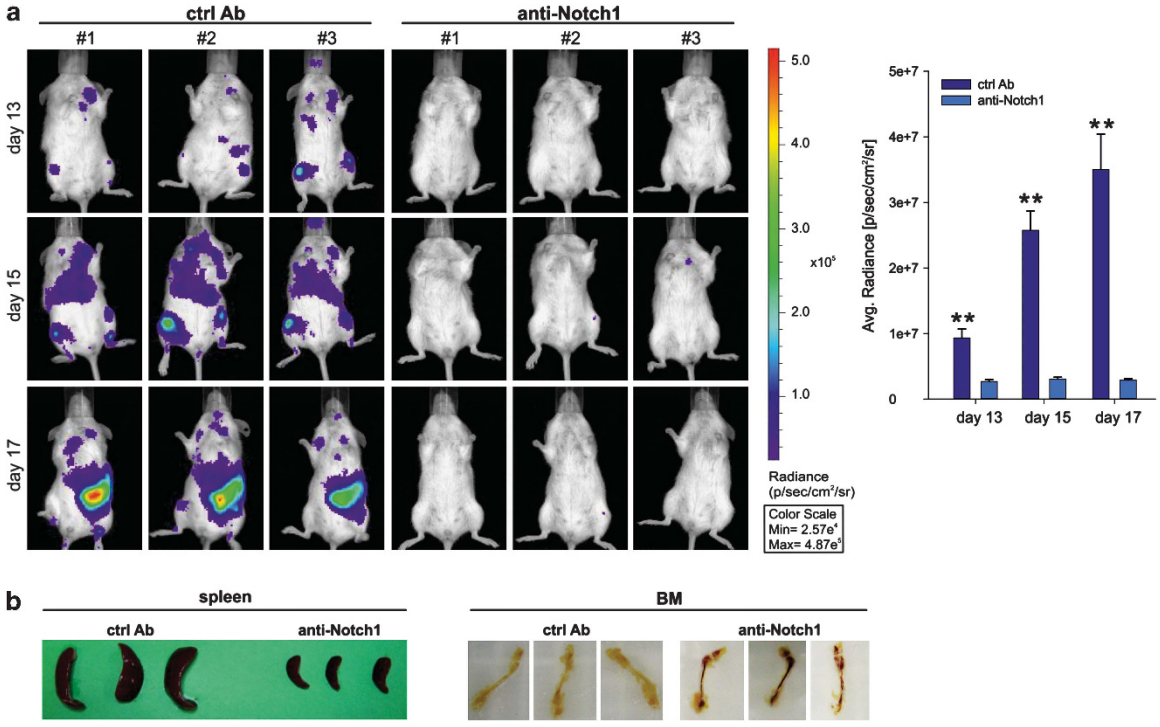

Figure 2. Anti-Notch1 reduces tumor burden in mice bearing human T-ALL cells. (**a**) Tracking leukemia outgrowth by optical imaging. PDTALL19 cells were labeled with the luciferase gene and i.v. injected into NOD/SCID mice (5×10^6 cells/mouse; $n = 5$ mice/group). Left panel: Representative images acquired at day 13, 15, 17 of three representative control (ctrl) or anti-Notch1-treated mice. Right panel: Quantitative analysis of luciferase activity at various time points of measurement ($n = 5$ mice/group). Statistically significant differences in average radiance in the two groups of samples are indicated (**$P < 0.001$). (**b**) Macroscopic features of the spleens and femurs from ctrl or anti-Notch1-treated mice. Leukemia outgrowth is accompanied by splenomegaly and pale appearance of the BM, two pathological features which are lacking in anti-Notch1-treated mice.

primary samples that engrafted and those that did not engraft (not shown). Molecular analysis disclosed that all xenografts maintained the same T-cell receptor rearrangement found in the primary leukemia cells from patients (Table 1) and had heterogeneous *NOTCH1* and *FBW7* genetic status. Altogether, 12 samples (63.2%) carried *NOTCH1* mutations, including mutations in the HD domain ($n = 7$), the PEST (proline-glutamic acid-serine-threonine-rich domain) domain ($n = 3$), HD + PEST ($n = 1$) or HD + TAD ($n = 1$). *FBW7* mutations were found in $n = 4$ samples (PDTALL 1, 4, 10 and 19) bearing also Notch1 HD mutations. Finally, $n = 7$ xenografts had wild-type *NOTCH1* and *FBW7* sequences (Table 1). Additional data on patient's age, the phenotype, the MRD class risk and prednisone sensitivity are given in Table 1, whereas the diagnostic immunophenotype is shown in Supplementary Table II. Intriguingly, in most cases analyzed *NOTCH1* mutations correlated with expression levels of a set of canonical Notch-target genes, including *CR2*, *DTX1*, *HES1*, *NOTCH3* and *pTα* (Supplementary Figure S3), indicating that these mutations lead to sustained activation of the pathway. Exceptions were PDTALL6 and PDTALL18, two xenografts with relatively sustained Notch signaling in the absence of mutations in the exons tested, and PDTALL21, a xenograft with quite low Notch signaling notwithstanding an HD mutation.

Based on these findings, we sought to investigate whether Notch1 genetic status was a predictive factor of response to Notch-targeted therapy. To this end, four xenografts bearing *NOTCH1* mutations (PDTALL8, 11, 12 and 19) and three xenografts with wild-type *NOTCH1* sequences (PDTALL13, 16 and 18)—all but PDTALL12 derived from either high MRD risk patients or prednisone poor responders—were selected to investigate the therapeutic efficacy of anti-Notch1 OMP-52M51.

Therapeutic effects of anti-Notch1 therapy in T-ALL models

Initially, early intervention trials were carried out. These involved weekly i.p. injection of anti-Notch1 mAb or a control mAb starting from 2 days after i.v. injection of T-ALL cells and extending up to the killing of mice, i.e. 14–29 days after T-ALL cell injection (Figure 1a). Human CD5 and CD7, two surface markers highly expressed by the T-ALL xenografts as well as by the matched primary cells (Supplementary Table SII), were used to track leukemia engraftment by flow cytometry. Evaluation of T-ALL cells in the first blood drawings from mice at day 9 showed a slight reduction in circulating leukemia cells in treated versus control mice in five out of the seven xenografts analyzed (PDTALL8, 11, 12, 19 and 13) and comparable numbers in the other two xenografts (PDTALL16, 18), suggesting that anti-Notch1 therapy did not substantially compromise initial engraftment of T-ALL cells in mice (Figure 1b). At killing, however, significantly lower levels of human $CD7^+$ cells were found in the blood, BM and spleen of anti-Notch1-treated PDTALL8, 11, 12 and 19 mice, compared with controls (Figure 1b). Results were confirmed by measurement of human $CD5^+$ cells as additional read-out of residual leukemia cells in mouse organs (Supplementary Figure S4). Moreover, a clear reduction in surface CD7 expression was also measured in these samples, whereas CD5 levels were not down-modulated (Supplementary Figure S5). Importantly, therapeutic response matched the Notch1 genetic status of the T-ALL xenografts: *NOTCH1* mutations in PDTALL8, 11, 12 and 19 cells correlated with good response to anti-Notch1 therapy. In contrast, PDTALL13, 16 and 18 xenografts formed by T-ALL cells with wild-type Notch1 receptors were substantially resistant to Notch1 blockade (Figure 1b).

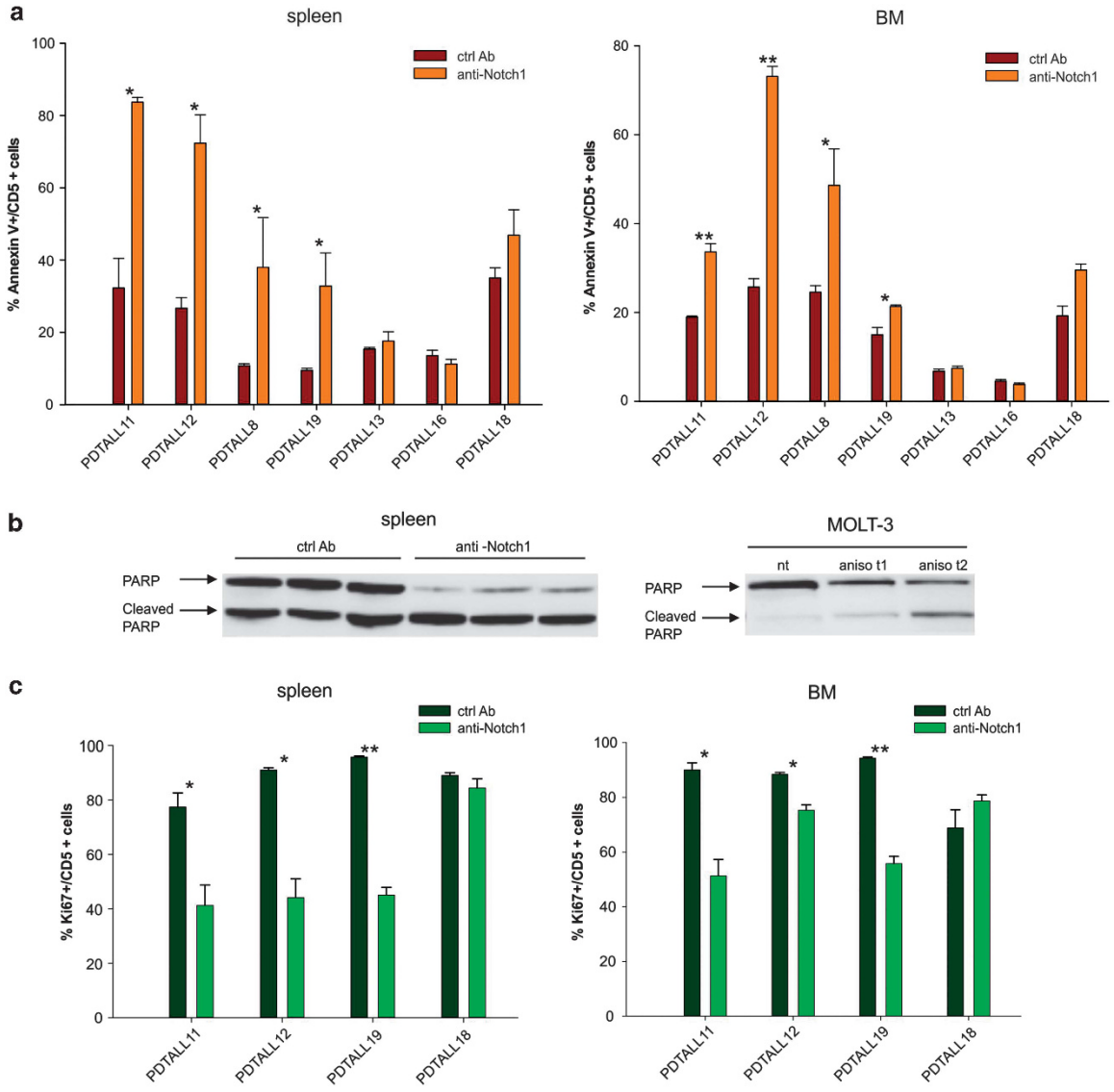

Figure 3. Anti-Notch1 therapy increases apoptosis and reduces proliferation of T-ALL cells. (**a**) At killing, levels of apoptotic leukemic cells in the spleen (left panel) and in the BM (right panel) of control and anti-Notch1-treated mice were measured by annexin V labeling and flow cytometry ($n = 6$ mice/group). Statistically significant differences in the two groups of samples are indicated. (**b**) Analysis of PARP cleavage by western blot in three representative samples from the spleen (left panel) of PDTALL19 mice treated with either control Ab or anti-Notch1. MOLT-3 cells treated with the pro-apoptotic drug anisomycin (5 μM) for 90 (t1) or 210 min (t2) were used as positive control (right panel). (**c**) Evaluation of leukemic cell proliferation by flow cytometric analysis following staining with CD5 and Ki67 of T-ALL cells from the spleen or the BM of anti-Notch1-treated mice (*$P < 0.05$, **$P < 0.001$).

In view of these marked anti-tumor effects, we investigated whether Notch1 blockade could also improve survival. Mice bearing PDTALL12 or PDTALL19 cells were treated by weekly injections of anti-Notch1 mAb, starting 2 days after T-ALL cell injection. Compared with the control group, anti-Notch1 therapy extended survival of mice bearing PDTALL19 cells from 15 days to 44 days, whereas in the case of mice bearing PDTALL12 cells mean survival was >82 days (Figure 1c). These findings indicate that anti-Notch1 monotherapy can extend survival of the mice, but effects are heterogeneous, suggesting that intrinsic factors modulate therapeutic efficacy.

These findings were confirmed by optical imaging of tumor burden following labeling of PDTALL19 cells with a luciferase-expressing lentiviral vector: results show a >90% reduction in leukemia burden in anti-Notch1-treated mice at various time points of analysis (Figure 2a). At autopsy, the size of the spleen from anti-Notch1-treated PDTALL19 mice was markedly reduced compared with controls, and the femurs had a reddish appearance that contrasts with the pale femurs of control mice, reflecting massive infiltration and replacement of normal hematopoiesis by leukemia cells (Figure 2b).

Analysis of annexin V expression on leukemia cells from the spleen and BM of the mice disclosed significantly increased apoptosis of T-ALL cells following effective anti-Notch1 therapy (Figure 3a), which was also confirmed by analysis of PARP cleavage in cell lysates from the spleen (Figure 3b). Similarly, apoptosis of T-ALL cells was also markedly increased in the advance disease setting (not shown). Moreover, Ki67 staining disclosed a significant reduction of cell proliferation following anti-Notch1 mAb administration (Figure 3c), in agreement with the reported effects of Notch blockade in human T-ALL cells.[14]

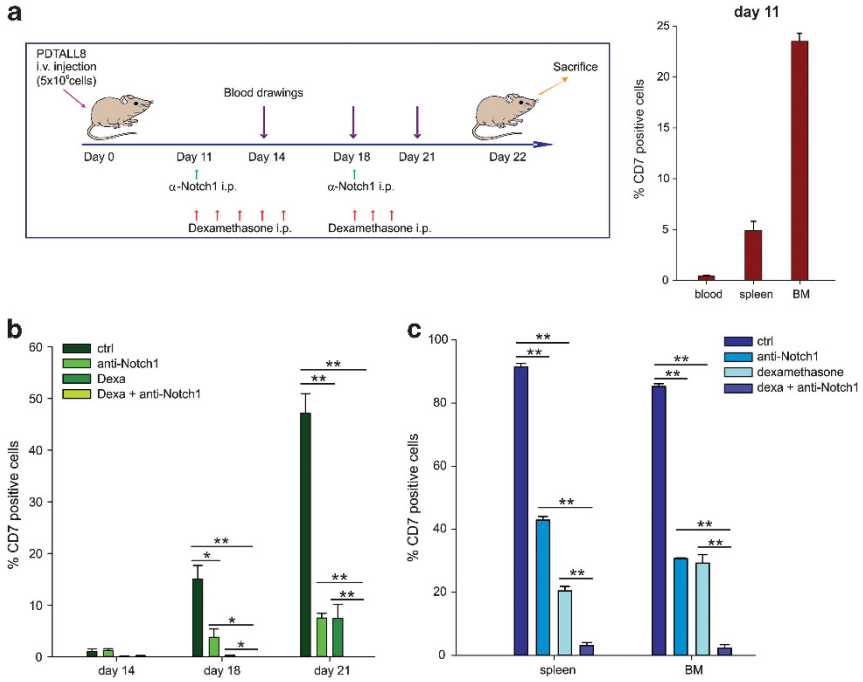

Figure 4. Synergistic effect of anti-Notch1 with dexamethasone in the advanced disease setting. (**a**) Outline of late intervention treatment with anti-Notch1 or control (ctrl) mAb in NOD/SCID mice ($n = 6$ mice/group) bearing PDTALL8 cells (left panel). Treatment was started 11 days after i.v. injection of T-ALL cells (5×10^6 cells/mouse), when leukemia cells were detected in the blood, spleen and BM of the mice (right panel, $n = 3$ mice/time point). Antibodies were subsequently administered at weekly intervals at 20 mg/Kg. Dexamethasone was administered daily at 10 mg/Kg (arrows). (**b**, **c**) Measurement of leukemia cells in the blood (**b**) or the spleen and BM (**c**) of mice at killing disclosed marked therapeutic effects. Statistically significant differences in the two groups of samples are indicated (*$P < 0.05$, **$P < 0.001$).

Anti-Notch1 therapy potentiates the *in vivo* effects of dexamethasone in an advanced disease model

To determine the efficacy of OMP-52M51 alone or in combination with drugs currently used for the treatment of T-ALL, NOD/SCID mice engrafted with PDTALL8 cells were treated with anti-Notch1 mAb, dexamethasone or a combination of anti-Notch1 with dexamethasone. To simulate an advanced disease setting, administration of the drugs started at day 11 after PDTALL8 cell injection, when mice were bearing ~5% leukemia cells in the spleen and >20% in the BM (Figure 4a). Mice received two injections of anti-Notch1 mAb on day 11 and on day 18 and/or dexamethasone (10 mg/Kg) daily from day 11 to day 15 and from day 18 until day 20 i.p. (Figure 4a). Treatment with either anti-Notch1 or dexamethasone significantly reduced the percentage of leukemic cells in the peripheral blood, (Figure 4b) BM and spleen (Figure 4c), but the effect was significantly greater in animals treated with the combination of the anti-Notch1 mAb with dexamethasone. These results show that anti-Notch1 therapy also has therapeutic efficacy in an advanced disease setting, and it has synergistic effects with other drugs used to treat T-ALL.

Anti-Notch1 therapy modulates the expression of Notch-target genes *in vivo*

To clarify whether these anti-leukemia effects were related to blockade of Notch signaling, we measured transcript levels of a set of Notch-target genes by TaqManArrays. Results show that anti-Notch1 therapy markedly attenuated the expression levels of most genes in the panel and particularly four genes (*CR2*, *DTX1*, *HES1* and *HES4*) in PDTALL19 xenografts, which bear Notch1 mutations and were treated with anti-Notch1 therapy starting 2 days after T-ALL cell injections in NOD/SCID mice (Figure 5a). Similar results were obtained with PDTALL8 xenografts (Figure 5b), although treatment was commenced at a more advanced stage (day 11, see Figure 4a). On the contrary, minimal effects were observed in PDTALL13 and PDTALL16 cells, bearing wild-type *NOTCH1* sequences (Figure 5c and data not shown). Some of these genes, such as *DTX1* and *HES4* or *NOTCH3*, were in fact undetectable in cells with wild-type *NOTCH1* sequences, suggesting that they might be considered sentinel genes for this pathway.

A global overview of the genes modulated by Notch1 blockade in PDTALL19 cells was obtained by gene expression profile (GEP) studies of RNA obtained from pools of T-ALL cells purified from the BM of mice treated with anti-Notch1 mAb or control mAb. Affymetrix arrays indicated markedly reduced expression levels of several canonical Notch-target genes, such as *CR2*, *HES1* and *NOTCH3* (Supplementary Table SIII)—generally fitting results of TaqManArrays—and further indicate that Notch1 blockade modulates expression of several transcripts involved in metabolic functions, such as glycolysis-associated genes (*PFKFB2*, *ALDOC*), membrane carriers (*SLC29A1*, *SLC16A6*, *SLC44A1*, *SLC1A4*, *SLC24A6*) and channels (*CLCA1*, *SCN3A*) (Supplementary Tables SIII and SIV). Gene set enrichment analysis (GSEA) was applied to the 'c2.all' MsigDB 3.0 collection of curated gene sets. We identified 36 up- and 374 downregulated gene sets (false discovery rate (FDR) q-value < 0.05). Interestingly, in the top list of downregulated gene sets we noticed several gene sets representing c-Myc targets, confirming the central role of c-Myc as an important mediator of Notch1 activity. Other interesting gene sets representing E2F1, YBX1 and TLX1 targets were also present among the 374 downregulated gene sets (not shown). GSEA analysis highlighted that the most relevant effects of anti-Notch1 on coordinated groups of genes were mainly in the sense of downregulation. Restricting our attention to KEGG (Kyoto Encyclopedia of Genes and Genomes) pathways, we identified 22 significantly down-regulated pathways (Supplementary Table SV) and no significant upregulated pathways with FDR q-value < 0.05. GSEA was also used to evaluate the significance of sets of genes, grouped

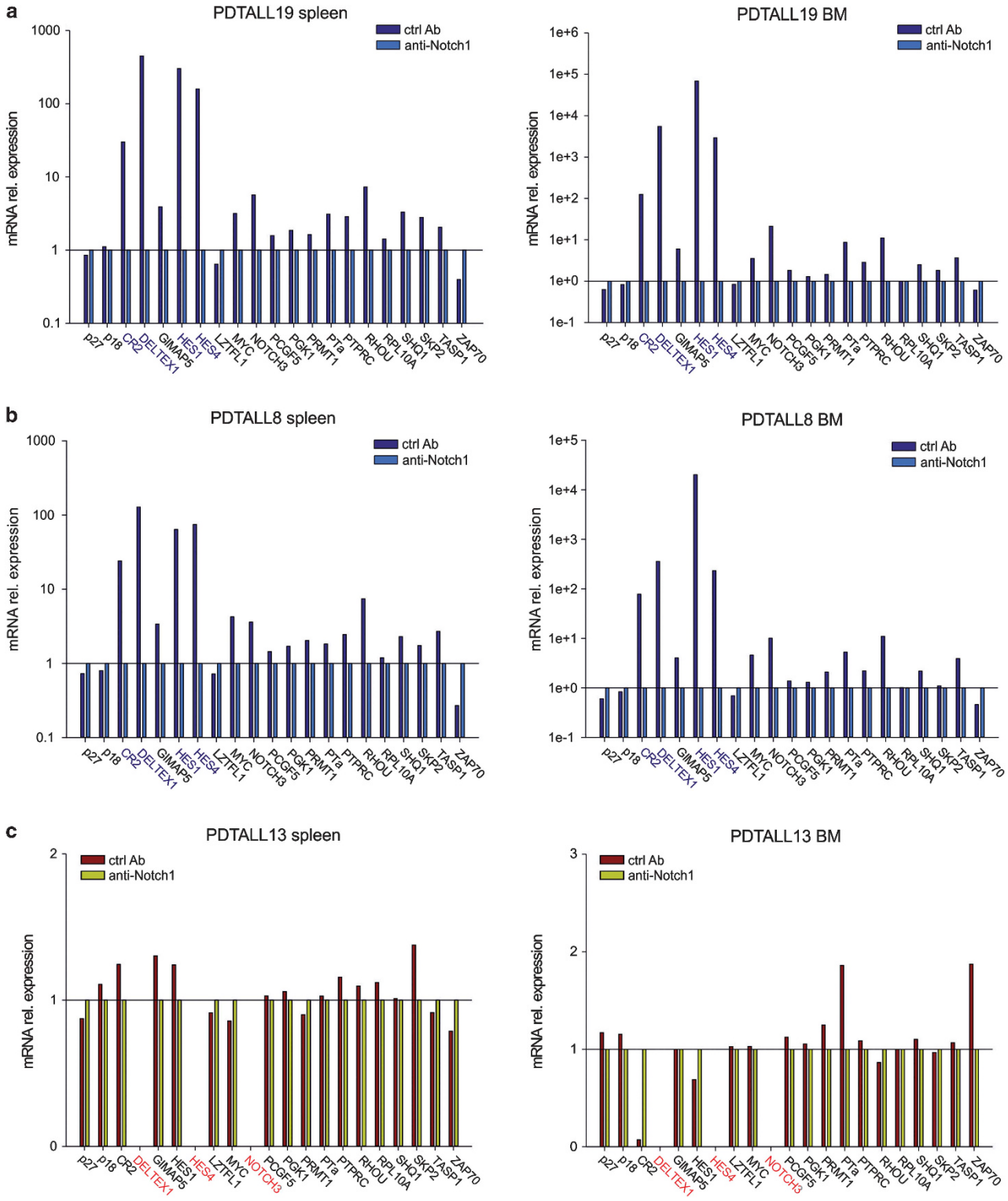

Figure 5. Anti-Notch1 therapy inhibits Notch signaling *in vivo*. Human CD5$^+$ cells were sorted from either the spleen or BM of anti-Notch1-treated or control mice, pooled ($n = 3$–6 samples per pool) and utilized to investigate effects on Notch signaling. Expression levels of 21 Notch-target genes were measured by TaqManArray Cards. (**a**) Gene expression profile in PDTALL19 xenografts, a representative example of anti-Notch1 good responder. Treatment—initiated by day 2—was highly effective in inhibiting the expression of Notch-target genes both in the spleen (left) and in the BM (right). (**b**) Gene expression profile in PDTALL8 xenografts, another anti-Notch1 good responder, in which therapy was started by day 11. (**c**) Gene expression profile in PDTALL13, a poor responder. The transcriptional profiles show that several Notch-related transcripts are barely detected in PDTALL13 cells and that their expression levels are minimally perturbed by anti-Notch1 therapy.

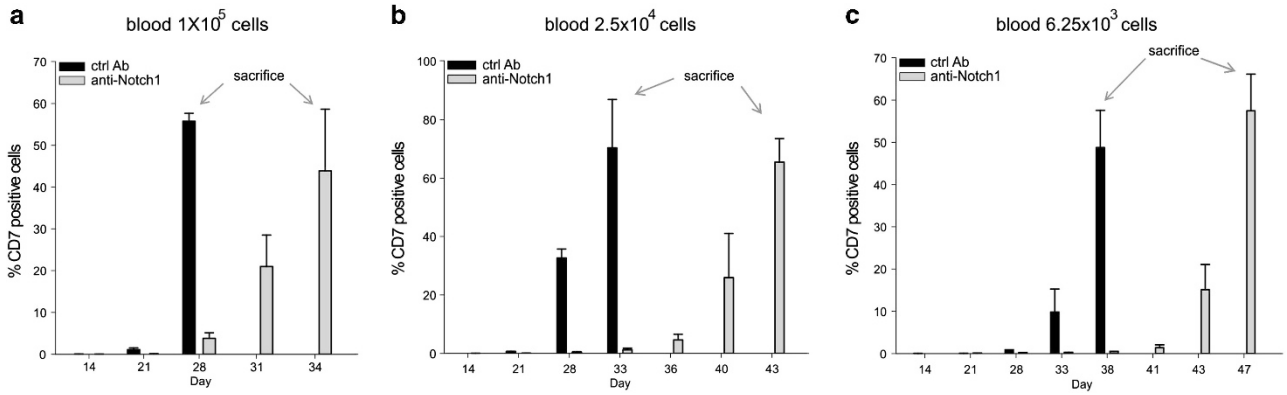

Figure 6. Anti-Notch1 therapy delays T-ALL engraftment in serial transplants (**a**-**b**). Measurement of circulating T-ALL cells in mice injected with serial dilutions of human Annexin $V^-/CD5^+$ cells (from 1×10^5 to 6.25×10^3 cells/mouse) sorted from the spleen of control (ctrl) and anti-Notch1-treated PDTALL19 xenografts ($n = 4$ mice/group).

together by biological process, as defined in the Gene Ontology, and we found enrichment of 12 gene sets again only in the sense of downregulation with FDR *q*-value <0.05 (Supplementary Table SV). Intriguingly, PET (positron emission tomography) studies disclosed that [^{18}F]FDG uptake, which is very high in PDTALL19 xenografts receiving the control antibody, was markedly reduced following treatment with anti-Notch1 mAb reaching uptake levels close to those observed in normal mice (Supplementary Figure S6). This reduction may reflect both reduction of tumor burden—as shown by other techniques—as well as some of the metabolic changes highlighted by GEP analysis.

Effect of anti-Notch1 therapy on leukemia-initiating cells (L-IC)

It has been proposed that ALL may arise from a transformation event in a primitive hematopoietic cell that has self-renewal ability to perpetuate the disease and may account for disease progression.[15–17] In T-ALL, previous studies found that $CD34^+CD4^-CD7^-$ cells might be enriched in L-IC;[18] however, other groups have proposed that the $CD34^+CD7^+$[19] or the $CD7^+CD1a^-$ subsets[20] might contain L-IC. To determine the effects of anti-Notch1 therapy on L-IC subset, we initially investigated by flow cytometry the presence of candidate L-IC cells by flow cytometry. Unfortunately, $CD34^+CD4^-CD7^-$ or $CD34^+CD7^+$ cells were almost undetectable ($<0.1\%$) in the xenografts used in this study, and their numbers did not change after anti-Notch1 therapy (data not shown). Therefore, to investigate whether efficacy of anti-Notch1 therapy was associated with reduction in the L-IC frequency, we quantified the tumorigenic potential of leukemia cells from regressing tumors by serial transplantation without making assumptions about tumorigenic sub-populations. To prevent bias due to the pro-apoptotic effects of anti-Notch1 therapy and cell sorting, Annexin $V^-/CD5^+$ T-ALL cells were FACS sorted from the spleen of mice bearing PDTALL19 cells after either two injections of anti-Notch1 or control mAbs and injected at three different doses (1×10^5, 2.5×10^4, 6.25×10^3) into naive NOD/SCID mice (4 mice/group). Mice injected with T-ALL cells from control Ab-treated mice developed full-blown leukemia within 28–38 days, depending on the number of T-ALL cells injected. By this time point, all mice injected with T-ALL cells from anti-Notch1-treated mice were apparently healthy and very low levels of leukemic cells were measured in their blood, although these mice eventually also developed leukemia 6–10 days later (Figure 6). These findings indicate that anti-Notch1 therapy not only reduces tumor growth during the treatment phase but also has a long-lasting effect on the T-ALL cells that impairs their ability to re-grow after serial transplantation, suggesting that anti-Notch1 also reduces L-IC frequency or function. Similar conclusions were also recently reported by another study.[21]

DISCUSSION

Efficient engraftment of primary tumor cells in mice is key to screen among targeted therapeutics, as recently shown for solid tumors.[22] Our study shows the feasibility of this approach also for pediatric T-ALL, an aggressive lymphoid malignancy with dismal prognosis in about 25% of patients. We utilized the model to investigate therapeutic activity of OMP-52M51, a novel anti-Notch1 antibody currently entering clinical trials. Notch-targeted therapies for T-ALL are not conceptually novel, but previous studies with anti-Notch1-specific mAb were largely limited to characterize activities of the therapeutic antibody on T-ALL cell lines either *in vitro*[10] or grown *in vivo* as subcutaneous tumor xenografts.[11] During preparation of this manuscript, therapeutic effects of another Notch1-specific mAb in T-ALL xenografts have been described.[21] The study by Ma *et al.*[21], however, was largely focused on L-IC subpopulations and other important issues such as therapeutic activity in poor prognosis T-ALL samples, mechanism of the therapeutic effect and identification of predictive biomarkers were not addressed. With respect to L-IC, in our study the xenografts that responded to anti-Notch1 therapy had negligible levels of $CD34^+$ cells, which precluded the possibility of confirming the key finding by Ma *et al.*[21] that Notch1-targeted therapy results in depletion of $CD34^+CD2^+CD7^+$ cells. On the other hand, it is known that T-ALL patient samples exhibit very variable proportions of $CD34^+$ blasts, ranging from $<1\%$ to up to 85% in the published studies,[19] indicating that this cell phenotype cannot be informative in all the cases. Importantly, however, the results of our serial transplantation experiment confirm that anti-Notch1 therapy impairs functional activity of L-IC cells, in line with other studies,[21,23] although their phenotype remains unidentified.

The OMP-52M51 mAb binds to the negative regulatory region of Notch1 and reduced Notch signaling in T-ALL cells bearing mutations in the HD/PEST domains as well as HD/TAD domains, showing that the antibody can prevent receptor auto-activation. It also worked in PDTALL11 and PDTALL12 xenografts, bearing a *NOTCH1* mutation in the HD and PEST domain, respectively, which might indicate that OMP-52M51 is able to block ligand-triggered activation of the Notch receptor, as also supported by results of luciferase activity in PC3 cells transfected with Notch1 expression constructs and cultivated in the presence of various Notch ligands (Supplementary Figure S1).

One important result of this study is the identification of candidate predictive markers of response. In fact, effective anti-Notch1 therapy correlated with marked impairment of the

transcript levels of Notch-target genes and with down-modulation of CD7 expression, which was also confirmed by GEP analysis. CD7, one of the galectin-1 receptors, is directly regulated by NF-κB upon T-cell activation.[24] As it is known that NF-κB is downstream of Notch1 in T-ALL cells,[25] it is tempting to speculate that reduced NF-κB activity following Notch1 blockade might account for reduced CD7 expression by the leukemia cells. However, we cannot exclude that reduced CD7 expression might depend on selective growth impairment of $CD7^+$ T-ALL cells by anti-Notch1 treatment, as it was reported that GSI specifically inhibit $CD7^+$ T-ALL cell growth *in vitro*.[19]

Overall, our results fit those obtained with targeted drugs for other malignancies,[26] underscoring that Notch-addicted samples might selectively profit by Notch-targeted therapy. With regard to the mechanism of the therapeutic effect, we found that anti-Notch1 therapy increased apoptosis and reduced proliferation of T-ALL cells *in vivo*, in line with the results of previous *in vitro* studies with GSI[2,27,28] and also with inhibition of Notch in murine T-ALL cell lines and primary tumors driven by transgenic ICN1.[5,29] We also found that anti-Notch1 therapy increased survival of treated mice, but the duration of response was remarkably different in PDTALL12 and PDTALL19 xenografts (Figure 1). This finding suggests that the type of *NOTCH1* mutation and/or additional genetic events in T-ALL cells could modulate the magnitude of response to Notch1-targeted therapy. In this respect, it has been shown that *FBW7* mutations could confer resistance to Notch inhibition by GSI.[30] Therefore it is tempting to speculate that *FBW7* mutations, found in PDTALL19 but not in PDTALL12 cells, could account for this difference in survival.

Notably, substantial numbers of viable leukemia cells (9–25%) were found in the BM or spleen of treated mice (Figure 3), and these cells were capable of inducing leukemia following serial transplantation (Figure 6), indicating that Notch1 mono-therapy needs to be supplemented. In previous studies, pharmacological interference with Notch signaling was shown to increase responses to dexamethasone, a leading drug in T-ALL treatment.[31] Along this line, we observed that anti-tumor effects of Notch1 blockade in T-ALL xenografts were further raised by combination with steroids (Figure 4). This could also lead to reduce duration of anti-Notch1 therapy in patients, thus preventing possible side effects of this targeted therapy on generation of T cells in the thymus, a physiological multi-step process tightly regulated by Notch1.[32]

Notch signaling is closely associated with regulation of cell metabolism through a feed-forward loop with c-Myc;[14] therefore it was not surprising to observe that anti-Notch1-treated mice had reduced levels of expression of c-Myc transcripts (Supplementary Table SIV) and strongly reduced levels of [^{18}F]FDG uptake compared with controls by PET analysis (Supplementary Figure S6). On the other hand, reduction of PET signals is partially explained by lower numbers of T-ALL cells infiltrating mouse organs, as shown by optical imaging and flow cytometry. These results confirm what was previously observed by Watanabe *et al.*[33] in a patient with T-ALL, suggesting the potential use of PET-[^{18}F]FDG for assessment of efficacy in clinical trials with Notch1-targeted therapy, particularly patients with solid tumors who lack alternative methods for rapid assessment of tumor responsiveness.

Finally, although recent advancements led to easier identification of poor prognosis T-ALL by phenotypic markers,[34,35] there is still a lack of effective therapies for this subset of patients. Our study clearly shows that *NOTCH1* mutations—a genetic feature which despite numerous studies has unclear prognostic relevance in the general population of T-ALL patients[36]—identifies a subset of high-risk T-ALL patients who might respond well to Notch-targeted therapy. In future studies, this approach—tested here with a prototypic signaling pathway in T-ALL—could also be extended to additional novel therapeutics and help to stratify patients and identify predictive biomarkers.

In addition to T-ALL, activating *NOTCH1* mutations have been shown to exist at significant frequencies and shown to be associated with poor clinical prognosis in other hematological malignancies, including chronic lymphocytic leukemia[37,38] and mantle cell lymphoma.[39] Thus, anti-Notch1 therapy, possibly combined with other cytotoxic drugs, may provide significant benefit to several types of leukemia and lymphoma patients with activating *NOTCH1* mutations.

CONFLICT OF INTEREST

FA, SS, AG and TH are employees, or former employees, and stockholders of OncoMed Pharmaceuticals. The other authors declare no conflict of interest.

ACKNOWLEDGEMENTS

We thank E Giarin (University of Padova) for immunophenotyping the T-ALL samples used in this study, E Rossi (University of Padova) for performing microarray hybridization and V Tosello and A Ferrando (Columbia University) for genetic analysis of *NOTCH1/FBW7* and critical reading of the manuscript. We also thank many people at OncoMed Pharmaceuticals who contributed to the generation and characterization of OMP-52M51, including Aaron Sato, Sasha Lazetic, Kellie Pickell and Timothy Velilla.

REFERENCES

1 Mansour MR, Linch DC, Foroni L, Goldstone AH, Gale RE. High incidence of Notch-1 mutations in adult patients with T-cell acute lymphoblastic leukemia. *Leukemia* 2006; **20**: 537–539.
2 Weng AP, Ferrando AA, Lee W, Morris 4th JP, Silverman LB, Sanchez-Irizarry C *et al.* Activating mutations of NOTCH1 in human T cell acute lymphoblastic leukemia. *Science* 2004; **306**: 269–271.
3 Dohda T, Maljukova A, Liu L, Heyman M, Grandér D, Brodin D *et al.* Notch signaling induces SKP2 expression and promotes reduction of p27Kip1 in T-cell acute lymphoblastic leukemia cell lines. *Exp Cell Res* 2007; **313**: 3141–3152.
4 Palomero T, Lim WK, Odom DT, Sulis ML, Real PJ, Margolin A *et al.* NOTCH1 directly regulates c-MYC and activates a feed-forward-loop transcriptional network promoting leukemic cell growth. *Proc Natl Acad Sci USA* 2006; **103**: 18261–18266.
5 Sharma VM, Calvo JA, Draheim KM, Cunningham LA, Hermance N, Beverly L *et al.* Notch1 contributes to mouse T-cell leukemia by directly inducing the expression of c-myc. *Mol Cell Biol* 2006; **26**: 8022–8031.
6 Weng AP, Millholland JM, Yashiro-Ohtani Y, Arcangeli ML, Lau A, Wai C *et al.* c-Myc is an important direct target of Notch1 in T-cell acute lymphoblastic leukemia/lymphoma. *Genes Dev* 2006; **20**: 2096–2109.
7 Wong GT, Manfra D, Poulet FM, Zhang Q, Josien H, Bara T *et al.* Chronic treatment with the gamma-secretase inhibitor LY-411,575 inhibits beta-amyloid peptide production and alters lymphopoiesis and intestinal cell differentiation. *J Biol Chem* 2004; **279**: 12876–12882.
8 Riccio O, van Gijn ME, Bezdek AC, Pellegrinet L, van Es JH, Zimber-Strobl U *et al.* Loss of intestinal crypt progenitor cells owing to inactivation of both Notch1 and Notch2 is accompanied by derepression of CDK inhibitors p27Kip1 and p57Kip2. *EMBO Rep* 2008; **9**: 377–383.
9 van Es JH, Clevers H. Notch and Wnt inhibitors as potential new drugs for intestinal neoplastic disease. *Trends Mol Med* 2005; **11**: 496–502.
10 Aste-Amézaga M, Zhang N, Lineberger JE, Arnold BA, Toner TJ, Gu M *et al.* Characterization of Notch1 antibodies that inhibit signaling of both normal and mutated Notch1 receptors. *PLoS One* 2010; **5**: e9094.
11 Wu Y, Cain-Hom C, Choy L, Hagenbeek TJ, de Leon GP, Chen Y *et al.* Therapeutic antibody targeting of individual Notch receptors. *Nature* 2010; **464**: 1052–1057.
12 Masiero M, Minuzzo S, Pusceddu I, Moserle L, Persano L, Agnusdei V *et al.* Notch3-mediated regulation of MKP-1 levels promotes survival of T acute lymphoblastic leukemia cells. *Leukemia* 2011; **25**: 588–598.
13 Kopan R, Ilagan MX. The canonical Notch signaling pathway: unfolding the activation mechanism. *Cell* 2009; **137**: 216–233.
14 Aster JC, Pear WS, Blacklow SC. Notch signaling in leukemia. *Annu Rev Pathol* 2008; **3**: 587–613.
15 Castor A, Nilsson L, Astrand-Grundström I, Buitenhuis M, Ramirez C, Anderson K *et al.* Distinct patterns of hematopoietic stem cell involvement in acute lymphoblastic leukemia. *Nat Med* 2005; **11**: 630–637.
16 Cox CV, Evely RS, Oakhill A, Pamphilon DH, Goulden NJ, Blair A. Characterization of acute lymphoblastic leukemia progenitor cells. *Blood* 2004; **104**: 2919–2925.

17 George AA, Franklin J, Kerkof K, Shah AJ, Price M, Tsark E *et al.* Detection of leukemic cells in the CD34(+)CD38(-) bone marrow progenitor population in children with acute lymphoblastic leukemia. *Blood* 2001; **97**: 3925–3930.
18 Cox CV, Martin HM, Kearns PR, Virgo P, Evely RS, Blair A. Characterization of a progenitor cell population in childhood T-cell acute lymphoblastic leukemia. *Blood* 2007; **109**: 674–682.
19 Gerby B, Clappier E, Armstrong F, Deswarte C, Calvo J, Poglio S *et al.* Expression of CD34 and CD7 on human T-cell acute lymphoblastic leukemia discriminates functionally heterogeneous cell populations. *Leukemia* 2011; **25**: 1249–1258.
20 Chiu PP, Jiang H, Dick JE. Leukemia-initiating cells in human T-lymphoblastic leukemia exhibit glucocorticoid resistance. *Blood* 2010; **116**: 5268–5279.
21 Ma W, Gutierrez A, Goff DJ, Geron I, Sadarangani A, Jamieson CA *et al.* NOTCH1 signaling promotes human T-cell acute lymphoblastic leukemia initiating cell regeneration in supportive niches. *PLoS One* 2012; **7**: e39725.
22 Bertotti A, Migliardi G, Galimi F, Sassi F, Torti D, Isella C *et al.* A molecularly annotated platform of patient-derived xenografts ("xenopatients") identifies HER2 as an effective therapeutic target in cetuximab-resistant colorectal cancer. *Cancer Discov* 2011; **1**: 508–523.
23 Tatarek J, Cullion K, Ashworth T, Gerstein R, Aster JC, Kelliher MA. Notch1 inhibition targets the leukemia-initiating cells in a Tal1/Lmo2 mouse model of T-ALL. *Blood* 2011; **118**: 1579–1590.
24 Koh HS, Lee C, Lee KS, Ham CS, Seong RH, Kim SS *et al.* CD7 expression and galectin-1-induced apoptosis of immature thymocytes are directly regulated by NF-kappaB upon T-cell activation. *Biochem Biophys Res Commun* 2008; **370**: 149–153.
25 Espinosa L, Cathelin S, D'Altri T, Trimarchi T, Statnikov A, Guiu J *et al.* The Notch/Hes1 pathway sustains NF-kappaB activation through CYLD repression in T cell leukemia. *Cancer Cell* 2010; **18**: 268–281.
26 Pao W, Chmielecki J. Rational, biologically based treatment of EGFR-mutant non-small-cell lung cancer. *Nat Rev Cancer* 2010; **10**: 760–774.
27 Lewis HD, Leveridge M, Strack PR, Haldon CD, O'Neil J, Kim H *et al.* Apoptosis in T cell acute lymphoblastic leukemia cells after cell cycle arrest induced by pharmacological inhibition of notch signaling. *Chem Biol* 2007; **14**: 209–219.
28 Palomero T, Barnes KC, Real PJ, Glade Bender JL, Sulis ML, Murty VV *et al.* CUTLL1, a novel human T-cell lymphoma cell line with t(7;9) rearrangement, aberrant NOTCH1 activation and high sensitivity to gamma-secretase inhibitors. *Leukemia* 2006; **20**: 1279–1287.
29 O'Neil J, Calvo J, McKenna K, Krishnamoorthy V, Aster JC, Bassing CH *et al.* Activating Notch1 mutations in mouse models of T-ALL. *Blood* 2006; **107**: 781–785.
30 O'Neil J, Grim J, Strack P, Rao S, Tibbitts D, Winter C *et al.* FBW7 mutations in leukemic cells mediate NOTCH pathway activation and resistance to gamma-secretase inhibitors. *J Exp Med* 2007; **204**: 1813–1824.
31 Real PJ, Ferrando AA. NOTCH inhibition and glucocorticoid therapy in T-cell acute lymphoblastic leukemia. *Leukemia* 2009; **23**: 1374–1377.
32 Radtke F, Wilson A, Mancini SJ, MacDonald HR. Notch regulation of lymphocyte development and function. *Nat Immunol* 2004; **5**: 247–253.
33 Watanabe N, Murakami J, Kameda K, Kato H, Kamisaki Y, Noguchi K *et al.* F-18 FDG-PET imaging in adult T-cell leukemia lymphoma. *Clin Nucl Med* 2008; **33**: 423–425.
34 Coustan-Smith E, Mullighan CG, Onciu M, Behm FG, Raimondi SC, Pei D *et al.* Early T-cell precursor leukaemia: a subtype of very high-risk acute lymphoblastic leukaemia. *Lancet Oncol* 2009; **10**: 147–156.
35 Zhang J, Ding L, Holmfeldt L, Wu G, Heatley SL, Payne-Turner D *et al.* The genetic basis of early T-cell precursor acute lymphoblastic leukaemia. *Nature* 2012; **481**: 157–163.
36 Sarmento LM, Barata JT. Therapeutic potential of Notch inhibition in T-cell acute lymphoblastic leukemia: rationale, caveats and promises. *Expert Rev Anticancer Ther* 2011; **11**: 1403–1415.
37 Fabbri G, Rasi S, Rossi D, Trifonov V, Khiabanian H, Ma J *et al.* Analysis of the chronic lymphocytic leukemia coding genome: role of NOTCH1 mutational activation. *J Exp Med* 2011; **208**: 1389–1401.
38 Villamor N, Conde L, Martinez-Trillos A, Cazorla M, Navarro A, Bea S *et al.* NOTCH1 mutations identify a genetic subgroup of chronic lymphocytic leukemia patients with high risk of transformation and poor outcome. *Leukemia* 2013; **27**: 1100–1106.
39 Kridel R, Meissner B, Rogic S, Boyle M, Telenius A, Woolcock B *et al.* Whole transcriptome sequencing reveals recurrent NOTCH1 mutations in mantle cell lymphoma. *Blood* 2012; **119**: 1963–1971.

Supplementary Information accompanies this paper on the Leukemia website (http://www.nature.com/leu)